RESEARCH ARTICLE

Development and Evaluation of Solidified Supersaturated SNEDDS Loaded with Triple Combination Therapy for Metabolic Syndrome

Abdelrahman Y. Sherif[1] · Doaa Hasan Alshora[1] · Mohamed Abbas Ibrahim[1] · Adel Jreebi[1]

Abstract

The present study aimed to develop and optimize solidified supersaturated self-nanoemulsifying drug delivery systems (SNEDDS) for the combined administration of antihypertensive, antihyperglycemic, and antihyperlipidemic drugs to enhance their solubility and dissolution during the treatment of metabolic syndrome. Various SNEDDS formulations were prepared and subjected to pharmaceutical assessment. The solubility of candesartan (CC), glibenclamide (GB), and rosuvastatin (RC) in SNEDDS and supersaturated SNEDDS formulations was evaluated. The optimized formulation was solidified using Syloid adsorbent at different ratios. Pharmaceutical characterization of the formulations included particle size, zeta potential, *in-vitro* dissolution, PXRD, FTIR, and SEM analysis. The prepared optimized formulation (F_6) was able to form homogeneous nanoemulsion droplets without phase separation, which is composed of Tween 20: PEG-400: Capmul MCM (4: 3: 3). It was mixed with 5% PVP-K30 to prepare a supersaturated liquid SNEDDS formulation (F9). In addition, it was found that the addition of PVP-K30 significantly increased solubility CC and GB from 20.46 ± 0.48 and 6.73 ± 0.05 to 27.67 ± 1.72 and 9.45 ± 0.32 mg/g, respectively. *In-vitro* dissolution study revealed that liquid and solid SNEDD formulations remarkably improved the dissolution rates of CC, GB, and RC compared to pure drugs. XRPD and FTIR analysis revealed that all drugs present in an amorphous state within prepared solidified supersaturated SNEDDS formulation. SEM images showed that liquid SNEDDS formulation was successfully adsorbed on the surface of Syloid. Overall, optimized F9 and solidified supersaturated SNEDDS formulations showed superior performance in enhancing drug solubility and dissolution rate. The present study revealed that the proposed triple combination therapy of metabolic syndrome holds a promising strategy during the treatment of metabolic syndrome. Further *in-vivo* studies are required to evaluate the therapeutic efficacy of prepared solidified supersaturated SNEDDS formulation.

Keywords candesartan · glibenclamide · metabolic syndrome · rosuvastatin · SNEDDS · triple therapy

Introduction

Metabolic syndrome, known as syndrome X, encompasses a collection of abnormal metabolic disorders, including elevated blood pressure, insulin resistance, hyperlipidemia, and central abdominal obesity [1]. These metabolic disturbances contribute to the manifestation of various medical conditions, notably type II diabetes mellitus, and coronary vascular disease [2]. The incidence of metabolic syndrome has promptly escalated in recent decades, particularly in modern countries. This surge is primarily attributed to increased diet intake rich in calorie content and low physical activity due to the availability of mechanical transportation and motionless activities [3, 4]. Furthermore, smoking, alcohol consumption, and stress conditions exacerbate the occurrence of metabolic syndrome [5]. Therefore, lifestyle modification should be implemented in terms of consuming a diet with a high fiber content and increasing physical activity [2, 6].

The National Institutes of Health (NIH) recommends starting combinational administration of pharmacotherapies to lower blood pressure, glucose, and lipid level [7]. Therefore, combinational therapeutic molecules, including antihypertensive agent (angiotensin-converting enzyme inhibitors or angiotensin receptor blockers), antihyperglycemic agent (sulfonylurea), and antihyperlipidemic agent (statins), are usually prescribed to maintain normal level of blood pressure, glucose, and lipid levels, respectively [8, 9].

✉ Abdelrahman Y. Sherif
ashreef@ksu.edu.sa

1 Department of Pharmaceutics, College of Pharmacy, King Saud University, 11451 Riyadh, Saudi Arabia

🖄 Springer

Candesartan is a potent long-lasting antihypertensive agent that exerts its pharmacological action through blocking the angiotensin II receptor [10, 11]. It has been reported that angiotensin II receptor could have a superior edge over angiotensin-converting enzyme inhibitors in the protection of systemic organs [12]. A clinical study showed that candesartan was able to restore blood pressure to normal level in diabetic patients with a protective effect against renal injury [13]. Moreover, the angiotensin II receptor present in adipose tissue triggers insulin resistance and glucose intolerance. Therefore, the administration of angiotensin II receptor like candesartan enhances normal metabolic body activities [14].

Glibenclamide (GB) is an antihyperglycemic drug that belongs to the sulfonylurea group [15, 16]. GB exerts its antidiabetic activity through increasing insulin secretion. This is achieved following the inhibition of ATP-dependent potassium channels present in the beta cell of the pancreas [17]. Franco *et al*. found that early treatment with GB in pre-diabetic obese male rats prevented the onset of obesity, reduced fat tissue accumulation, and lowered glycemia [18].

Rosuvastatin reduces cholesterol blood levels through competitive inhibition of 3-hydroxy-3-methylglutaryl CoA reductase [19, 20]. Various clinical studies showed that rosuvastatin has a superior antihyperlipidemic activity over other statins for patients diagnosed with metabolic syndrome [21, 22]. Furthermore, Bostan *et al*. reported that rosuvastatin exhibited notable positive impacts on atherogenic dyslipidemia, inflammatory biomarkers, and oxidative stress among individuals diagnosed with Metabolic Syndrome [23].

However, the major limitation of multiple administrations of medication pills is low adherence of patients and compliance which could result in ineffective therapy [24]. Consequently, mixing the three therapeutic agents in a single pharmaceutical dosage form could resolve the aforementioned limitation of multiple pill administration. Moreover, the absolute oral bioavailability of candesartan, glibenclamide, and rosuvastatin are about 40, 45, and 20%, respectively [25–27]. Therefore, triple metabolic syndrome therapy should be formulated using a drug delivery system that is able to enhance drugs solubility and bioavailability [28, 29].

Different classes of drug delivery systems have been designed to boost the oral bioavailability of poorly water-soluble drugs [30]. Among them, a self-nano-emulsifying drug delivery system (SNEDDS) was extensively employed to overcome the limited solubility of lipophilic drugs. This can be ascribed to its durable colloidal stability, enhanced drug permeability through the mucosal membrane, improved drug bioavailability, and applicability in manufacturing and scaling up [31, 32].

The present study aimed to prepare SNEDDS formulation loaded with triple therapy to enhance therapeutic outcomes and patient compliance. To achieve this, various formulations were prepared and assessed in terms of emulsification and drug solubility. Furthermore, supersaturated SNEDDS formulation was prepared to enhance drug loading capacity and subjected to solidification using Syloid adsorbent. After that, solidified supersaturated SNEDDS formulation was subjected to *in-vitro* dissolution, PXRD, SEM, and FTIR studies for pharmaceutical characterization.

Materials and Methods

Materials

Candesartan cilexetil and Glibenclamide were generously provided by Riyadh Pharma (Riyadh, Saudi Arabia) and SPIMACO (Qassim, KSA), respectively. Rosuvastatin calcium was acquired from Beijing Mesochem Technology Co., Ltd. (Beijing, China). Kolliphor-EL (K-EL, surfactant), Kollidon® K30 (PVP-K30), and Kollisolv PEG 400 (PEG-400, co-surfactant) were acquired from BASF (Ludwigshafen, Germany). Tween-20 (T-20, surfactant) was supplied by BDH (England). Span-80 (S-80, co-surfactant) was purchased from Merck (Darmstadt, Germany). Capmul MCM (CMCM, oil) was obtained from Abitec Corporation (Janesville, USA). Oleic acid (OA, oil) was acquired from Avonchem (Cheshire, UK).

Preparation of SNEDDS Formulation

Table I shows the excipient composition used to prepare drug-free SNEDDS formulations. The mentioned ingredients were added and then subjected to vigorous agitation using a vortex mixer to ensure the homogeneity of SNEDDS components [33]. Subsequently, the resulting SNEDDS formulations were assessed using diverse characterization procedures to identify the most promising formulations for subsequent pharmaceutical testing.

Preparation of Supersaturated SNEDDS (Sup-SNEDDS) Formulation

A preliminary solubility screening of different types of polymers (Poloxamer 407, PVP-K30, and HPMC) was performed to select the optimum precipitation inhibitor. Firstly, 100 mg of the used polymer was blended with 1900 mg of the SNEDDS in a 10 mL glass beaker to prepare a final concentration of 5 w/w%. The prepared mixture was exposed to mixing at 1000 rpm using a magnetic stirrer for 24 h. Finally, the soluble polymer was chosen depending on the clarity of SNEDDS' physical appearance.

Table I Composition of Drug-free SNEDDS Formulations

Formulation code	Surfactant		Co-surfactant		Oil	
	Kolliphor-EL	Tween-20	PEG-400	Span-80	Oleic acid	Capmul MCM
F1	400		300		300	
F2	400		300			300
F3	400			300	300	
F4	400			300		300
F5		400	300		300	
F6		400	300			300
F7		400		300	300	
F8		400		300		300

Preparation of Solidified Supersaturated SNEDDS

To prepare the drug-loaded liquid supersaturated SNEDDS formulation, 8 mg of candesartan cilexetil, 2.5 mg of gliben-clamide, and 5 mg of rosuvastatin calcium were accurately weighed and dissolved in every 500 mg of the SNEDDS formulation. After that, solidified supersaturated SNEDDS was formulated utilizing Syloid adsorbent. Drug-loaded liquid supersaturated SNEDDS formulation was mixed with Syloid at various ratios (1:0.5, 1:0.75, 1:1, and 1:1.25) to prepare S1, S2 and S3 formulations, respectively [34].

Miscibility test

This test was performed to observe the incident of phase separation and check the miscibility of SNEDDS components. Following SNEDDS preparation, it was exposed to centrifugation for 10 min at a speed of 14,000 rpm at a controlled room temperature ($22.0 \pm 2.0°C$). This accelerates the separation of immiscible components from each other. Following the centrifugation process, the SNEDDS formulations in the Eppendorf tubes were visually inspected to evaluate their uniformity [35].

Emulsification Test

An emulsification test was performed to ensure the ability of the surfactant and co-surface to form an emulsification system without oil separation. This is attained following the dilution of SNEDDS with water (1:1000) and mixing with a magnetic stirrer for 5 min at 250 rpm. After that, a visual inspection of the dispersed system was checked to assess its physical appearance [36].

Physicochemical Characterization

The physicochemical properties of the SNEDDS formulations were assessed through various analyses. The particle size and zeta potential of the dispersed formulations were determined using a Zetasizer instrument. The results were reported as the average of three measured values for each formulation [37].

Solubility Test

A solubility test was conducted to investigate the solubility of each drug individually in the SNEDDS formulations. During the experiment, excess amounts of CC, GB, and RC were gradually added to the SNEDDS formulations (F2, F6, and Sup-F6) in a 4 mL glass vial. The mixture was then stirred using a magnetic stirrer at 1000 rpm for 24 h. Afterward, the mixture was centrifuged at 14,000 rpm for 10 min to precipitate the undissolved drug. An accurately weighed amount from the supernatant was carefully weighed in an Eppendorf tube. Acetonitrile was added to the formulation and exposed to sonication, guaranteeing the ability to extract the drug. The extracted solution was appropriately diluted and analyzed against a constructed calibration curve to determine the drug concentration [35].

In-Vitro Dissolution Study

The dissolution behavior of the drugs was determined by utilizing USP apparatus II. The condition of the test was adjusted using phosphate buffer pH 6.8 with a fixed temperature of $37 \pm 0.5°C$. The paddle was rotated at 75 rpm. An amount equivalent to 2.5 mg GB, 5 mg RC, and 8 mg of CC was calculated for the selected liquid SNEDD, and the solidified formulations. At preplanned times of 5, 15, 30, and 60 min, 5 ml samples were withdrawn and analyzed using the UPLC method [38].

PXRD

Assessment of crystallinity of the three tested drugs in their solidified SNEDDS formula was evaluated using XRPD

studies. Briefly, an Ultima IV x-ray diffractometer (Rigaku Inc., Tokyo, Japan) was used. The diffractometer operated Cu Kα radiation for X-ray measurements. The XRPD spectra were attained by scanning the samples over a range of 2θ range of 5–60° to allow the detection of diffraction peaks related to the crystallographic structures present in the samples [39].

FTIR

The FTIR scans for the individual APIs, Syloid and the solidified SNEDD formul were performed by using FTIR spectrophotometer instrument (Perkin Elmer, MA, USA). Solid powder samples were mixed with potassium bromide (a spectroscopic grade), and compressed by hydraulic press into disks, which were then subjected to scanning from 4000 to 400 cm^{-1}. The data were then analyzed using Perkin Elmer software (Spectrum V5.3.1) [35].

SEM

The pure APIs and optimum solidified SNEDDS formula were investigated for their surface properties and their globule size after solidification using scanning electron microscopic (SEM). Regarding SEM analytical measures, the powder sample was sputter-coated with a thin layer of gold–palladium. Thereafter, the coated samples were scanned at a voltage of 60 mV in order to confirm appropriate imaging settings and permit obtaining comprehensive information for the particles' surface morphology [40].

Results and Discussion

Evaluation of Drug-Free SNEDDS Formulation

Table II presents the results obtained from the miscibility and emulsification test of the developed formulations. The present results showed that the used components are miscible with each other with no sign of phase separation. However, the F1 formulation was incapable of being dispersed in the medium, resulting in the development of aggregated particles, as shown in Fig. 1. Furthermore, upon dispersion of F3-F5, F7, and F8 formulations, it was observed that the oil failed to be incorporated into the dispersed emulsion, and macroparticles were clearly observed by the eye in the medium (Fig. 1). In contrast, only the F2 and F6 formulations were able to form nanoemulsion droplets with a transparent appearance and without any signs of phase separation (Fig. 1). This could be explained by the optimal HLB values between combined SNEDDS components that form nanoemulsion droplets. Regarding surfactants, Tween 20 and Kolliphor-EL have HLB values between 14 – 17 [41].

Table II Evaluation of Drug-free SNEDDS Formulation

Formulation code	Miscibility	Physical appearance of dispersed SNEDDS formulation	Evaluation
F1	✓	Indispensable system	x
F2	✓	Transparent	✓
F3	✓	Phase separation	x
F4	✓	Phase separation	x
F5	✓	Phase separation	x
F6	✓	Transparent	✓
F7	✓	Phase separation	x
F8	✓	Phase separation	x

For oils, capmul MCM has an HLB value of 4.7 [42], while oleic acid has an HLB value of 1.2 [43]. Therefore, it could be observed that HLB value of capmul MCM was closer to HLB of surfactants than oleic acid. This enhances the emulsification tendency of the dispersed system containing capmul MCM compared to its counterpart containing oleic acid. Regarding co-surfactant, the SNEDDS formulation containing PEG-400 successfully formed a nanoemulsion owing to its reported emulsifying properties, which reduce the interfacial tension between the surfactant and oil [44]. Therefore, F2 and F6 were selected due to the visualized transparent physical appearance of the dispersed system in Fig. 1.

The particle size, PDI, and zeta potential of the successful SNEDDS formulations (F2, and F6) were measured and reported in Table III. The results showed that F2 and F6 formulations were able to form a nano-dispersion system with a negative zeta potential value. The current findings showed that the prepared SNEDDS could enhance the bioavailability of the incorporated drug molecules [45–47]. Additionally, the presence of residual fatty acids in oils could be responsible for the measured negative zeta potential value, which aligns with previously published data [48]. Furthermore, various studies showed that negatively charged nanoparticles enhanced the oral bioavailability of payload drugs [49, 50]. Therefore, prepared SNEDDS formulation is anticipated to significantly boost the oral bioavailability of loaded triple therapy during the treatment of metabolic syndrome.

Solubility study was conducted to investigate the loading capacity of triple therapy in F2 and F6 formulations. The solubility of CC, GB, and RC in F2 and F6 formulations was determined to be (20.14 ± 0.54 and 20.46 ± 0.48 mg/g), (6.23 ± 0.04 and 6.73 ± 0.05 mg/g), and (198.89 ± 4.03 and 269.78 ± 11.38 mg/g) respectively, as illustrated in Fig. 2. These results indicate that F6 significantly enhances the solubility of GB and RC while having no significant impact on CC solubility when compared to F2. Therefore, F6 formulation was picked as the leading formulation.

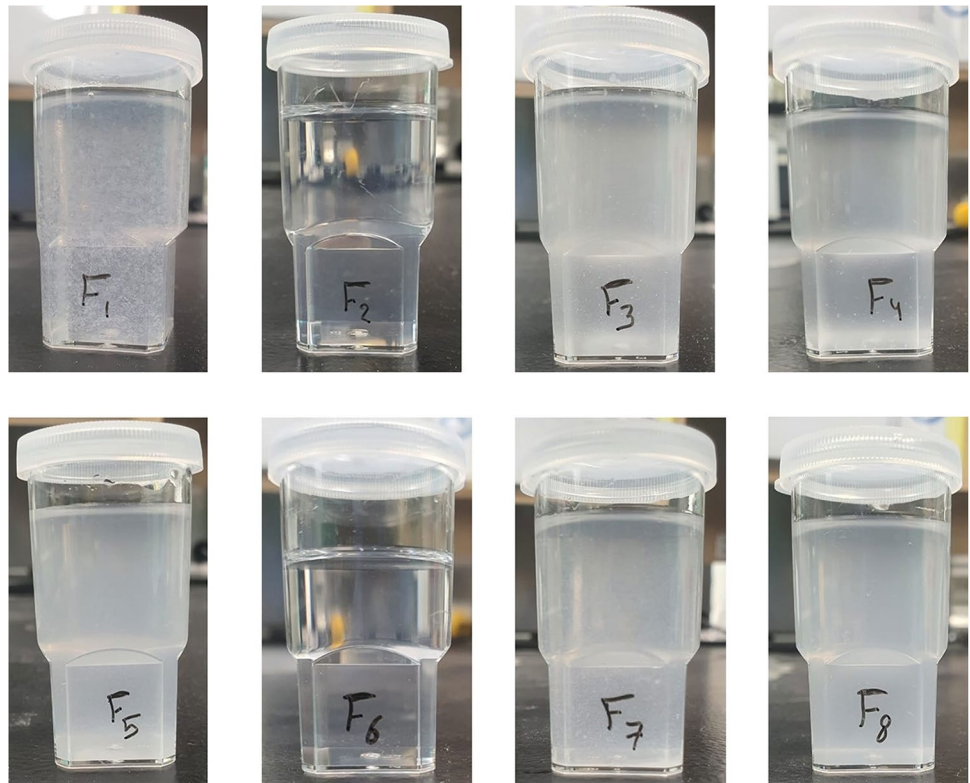**Fig. 1** Physical Appearance of Dispersed SNEDDS Formulations

Table III Particle size, PDI, and Zeta Potential Values of SNEDDS Formulations

Formulation code	Particle size (nm)	PDI	Zeta potential (mV)
F2	138.7 ± 3.2	0.513 ± 0.017	- 18.3 ± 1.3
F6	148.0 ± 3.2	0.531 ± 0.026	- 30.8 ± 1.2
F9 (F6 supersaturated with PVP)	123.9 ± 2.4	0.512 ± 0.015	-22.5 ± 0.3
Drugs-loaded F9	99.5 ± 10.2	0.593 ± 0.011	- 30.4 ± 2.4
S1 (Solidified Drugs-loaded F9)	99.3 ± 0.8	0.583 ± 0.14	-29.7 ± 2.2
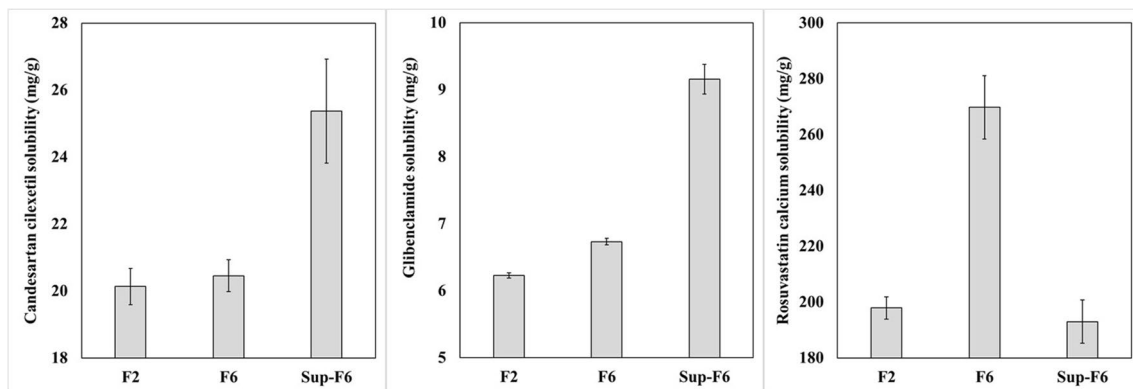
Fig. 2 Solubility of Candesartan cilexetil, Glibenclamide, and Rosuvastatin calcium in F2, F6, and Sup-F6 formulations

Evaluation of Supersaturated-SNEDDS Formulation

To enhance the solubility of CC and GB in F6 formulation, the solubility of various polymers (poloxamer 407, PVP K30, and HPMC) was investigated to prepare supersaturated SNEDDS. The current results showed that all polymers, except for PVP-K30, were unsuccessfully dissolved in SNEDDS formulations. This could be attributed to the capability of PVP to form bonds with used SNEDDS components, which facilitate its solubilization. Consequently, PVP-K30 was chosen to prepare supersaturated SNEDDS. Table III shows that the addition of PVP-K30 to the F6 formulation reduces the particle size of the dispersed F9 (F6 supersaturated with PVP) formulation from 148.0 to 123.9 nm. In addition, the solubility study revealed that the prepared F9 exhibited significantly higher solubility for CC and GB compared to the counterpart F6 (Fig. 2). The solubility of CC increased from 20.46 ± 0.48 to 27.67 ± 1.72 mg/g, while the solubility of GB increased from 6.73 ± 0.05 to 9.45 ± 0.32 mg/g. On the contrary, the solubility of RC was significantly decreased from 269.78 ± 11.38 to 193.03 ± 7.69 mg/g. This could be attributed to the increment in formulation viscosity owing to the presence of precipitation inhibitor polymer. Furthermore, dissolved RC during the experiment increased the viscosity of SNEDDS formulation. Both factors could hinder the movement of the stirrer during the solubility study and hinder the drug from dissolving. However, the remarkable measured value of RC solubility (193.03 mg/g), as well as the significant increase in CC and GB solubility in the F9 formulation, make it superior to the F6 formulation.

The F9 formulation was loaded with three drugs to prepare the Drugs-loaded F9 formulation. The emulsification test showed that the addition of the drug led to a significant decrease in particle size from 123.9 to 99.5 nm and zeta potential value from—22.5 to—30.4 mV. Even though most studies showed that drug loading increases dispersed nanoemulsion size, various studies have agreed with our findings. The previously published studies showed that drug addition to SNEDDS formulation resulted in the formation of smaller nanoemulsion droplets [51–53]. The observed change in particle size could be assigned to the interaction between loaded drugs and components within SNEDDS, which is in coordination with formerly published data in the literature [54]. In addition, the observed reduction in zeta potential value could be ascribed to possible interactions between the surfactant and one or more loaded drugs, with the drugs present on the surface of the dispersed nanoemulsion droplets [55]The detected change in zeta potential value is aligned with the particle size results, which indicate the presence of drug on the surface of dispersed nanoemulsion droplets. However, the dispersed system from the solidified Drug-Loaded F9 formulation has no significant alteration in the measured particle size and zeta potential values from the counterpart liquid formulation (Drug-loaded F9).

In-Vitro Dissolution

The dissolution profiles for CC, GB, and RC are presented in Fig. 3. The obtained results revealed that the percent of CC dissolved at the end of the experiment from liquid SNEDDS was significantly increased from 5.92 ± 1.49 to $60.79 \pm 3.48\%$ compared with the pure drug (Fig. 3a). The detected increase in the dissolution profile of CC from supersaturated liquid SNEDDS is ascribed to the solubilization effect produced by PVP and its capability to inhibit the precipitation of the drug [56]. The observed reduction in CC release from solidified SNEDDS could result from the retention of the drug in the porous structure of the adsorbent. This could be attributed to the precipitation of the drug within the pores of the adsorbent [57]. In contrast, the dissolution profile of GB and RC from solidified SNEDDS was almost similar to liquid SNEDDS, as seen in Fig. 3b and c, respectively. This could be ascribed to the intrinsic solubility of both drugs within SNEDDS components during the adsorption process. Therefore, nanoemulsion droplets with small particle sizes are freely formed owing to the exposure of a large surface area of solidified SNEDDS to dissolution media [58].

The percentage of GB dissolved from liquid SNEDDs at the end of the dissolution study was significantly increased to 60% compared to the pure API. For RC, the dissolution from both liquid and solidified SNEDDS is comparable to the pure RC, possibly due to the ionization of RC in the alkaline media. RC is a weak acid drug with high ionization in alkaline pH; thus, a high dissolution rate could be expected [59]. The initial dissolution rate after 5 min showed the superiority of liquid SNEDDS (89.24%) over the pure RC (72.12%). Among the solidified SNEDDS, formulation S3 has the highest dissolution rate over S1 and S2. This could be ascribed to the large surface area provided by adsorbing the drug on a higher ratio of Syloid, which leads to the detected increase in the dissolution rate of the drug. In addition, increasing the ratio of syloid could positively affect the powder's flowability and reduce the chance of powder caking and aggregation [34]. However, the S1 formulation was selected as the optimized formulation owing to its superiority in reducing the total dosage of the administered formulation.

PXRD

The crystalline natures of the three tested APIs (RC, GB, and CC) in their SNEDDS solidified by Syloid formula were traced by using XRPD spectra in comparison to the
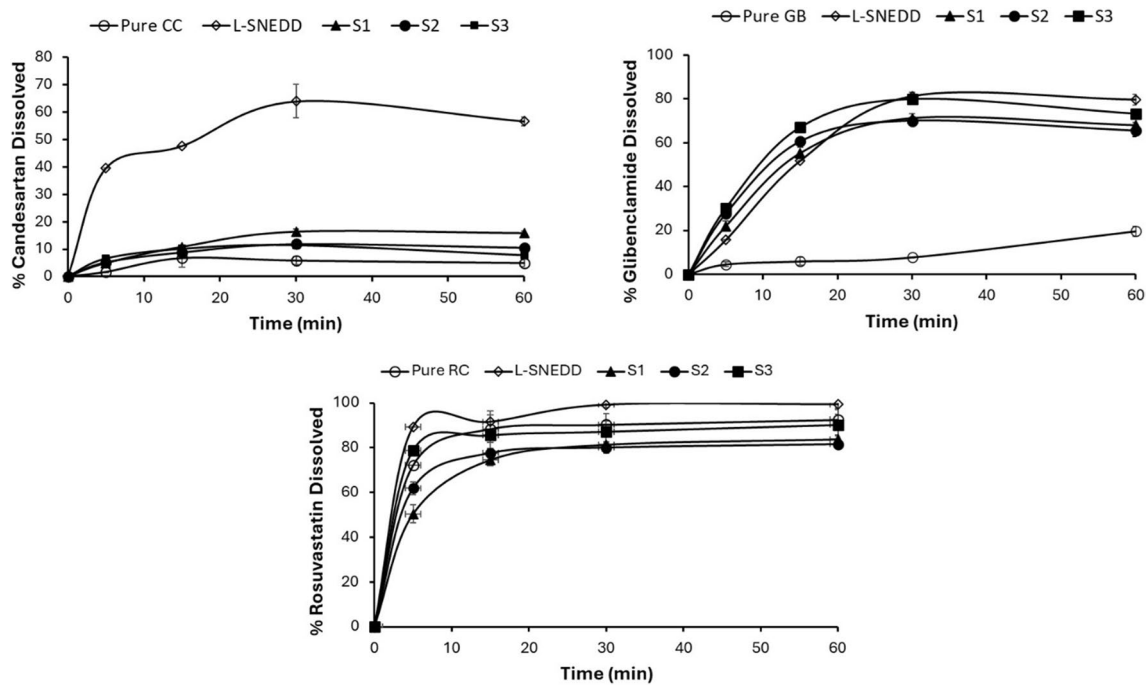
Fig. 3 Dissolution profiles of Candesartan, Glibenclamide, and Rosuvastatin

diffraction spectra of the individual components. The PXRD results are demonstrated in Fig. 4. The XRPD profile RC indicated the presence of a single diffraction peak at a 2θ degree of 31.8, revealing the lower crystallinity form of the
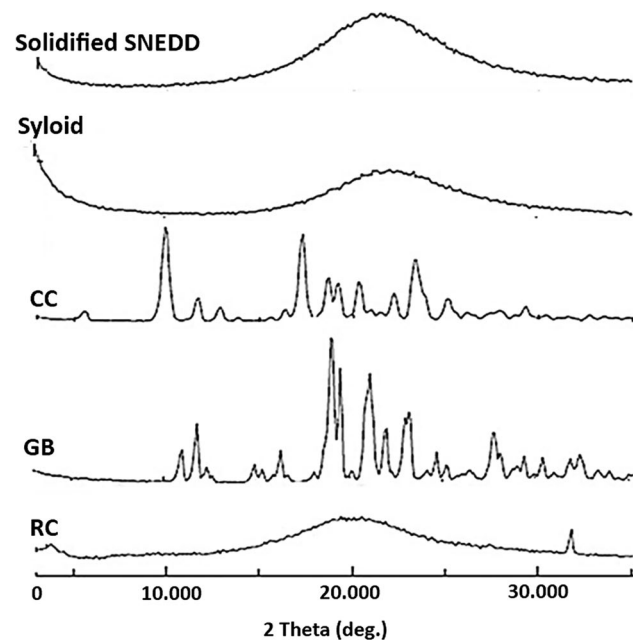

Fig. 4 XRPD spectra of SNEDDS formula containing RC, GB and CC and solidified with Syloid XDP 350 compared to the individual components

drug powder. In addition, different diffraction peaks with characteristic diffraction peaks appearing at diffraction angles of 2θ at 12.1, 18.9, 20.9, 23.2, 26.8, and 28.3 Å were detected in the spectrum of GB, indicating the existence of the drug in a crystalline form. Moreover, the spectrum of CC proves the crystallinity of the drug because of the presence of several diffraction peaks at 9.9, 17.3, 20.3, and 23.3 Å. In contrast, the SNEDDS solidifier (Syloid XDP 3050) indicated the absence of any diffraction peak in the X-ray spectrum. In the case of the solidified SNEDDS formula, all characteristic diffraction peaks of the tested drugs could not be detected in the XRPD spectra, specifying the dispersion of these APIs in the globules of the SNEDDS [60, 61].

FTIR

Figure 5 shows the FTIR spectra of the SNEDDS formula containing the three APIs (RC, GB, and CC) that was solidified with Syloid XDP 3050 (in a ratio of 1: 1.25) compared to the individual ingredients. The FTIR spectrum of RC showed a band a 3327 cm^{-1} that corresponds to carboxylic O–H stretching, a band at 2967 cm^{-1} for C-H stretching, and a band at 1545 cm^{-1} for C=O carbonyl stretching. GB FTIR spectrum denotes a forked intense band at 3362 and 3307 cm^{-1}, conforming to secondary N–H stretching. In addition, other bands were noticed at 1108 cm^{-1}, 1338 cm^{-1}, 1711 cm^{-1}, and 2853 cm^{-1}, matching to the symmetric SO2 stretching, asymmetric SO2 stretching, C=O amide, and

Fig. 5 FTIR spectra of SNEDDS formula containing RC, GB and CC and solidified with Syloid XDP 350 compared to the individual components
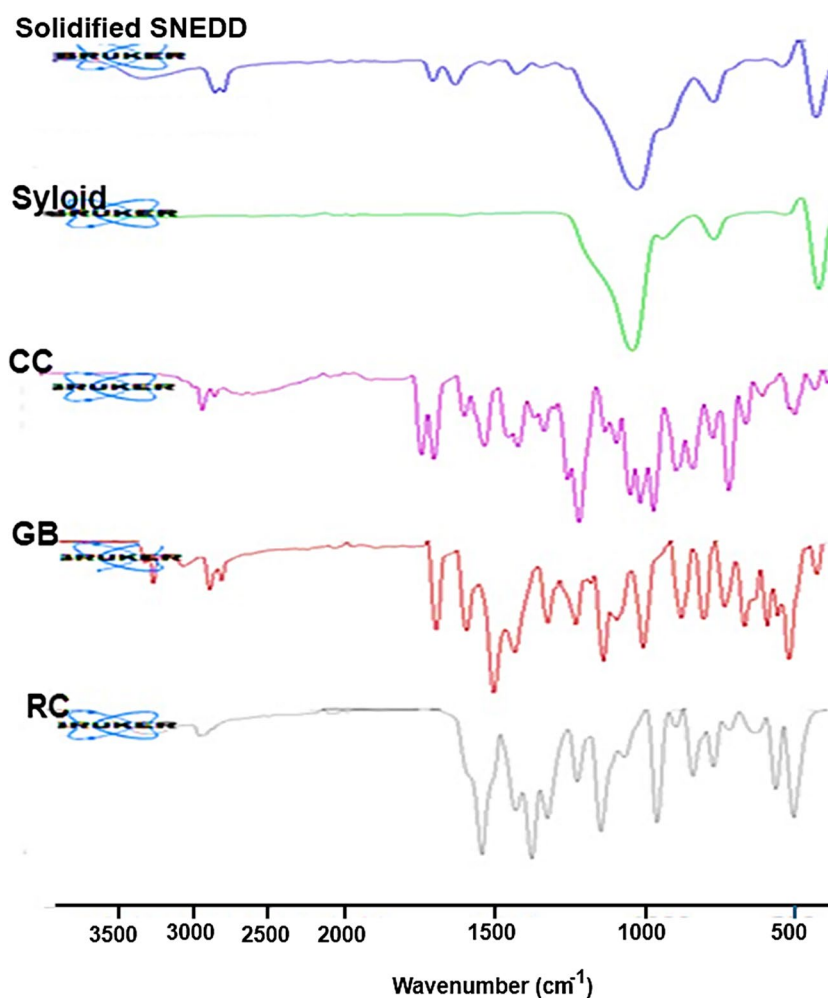
C-H, respectively. Moreover, the FTIR spectrum of CC indicated a strong -C-H stretching absorption band at 2939 cm-1, corresponding to the carbonyl C=O stretching at 1711 cm-1 and Strong C=O carbonyl stretching at 1751 cm^{-1}. The FTIR bands of the three APIs were in accordance of the reported data [62, 63]. In addition, the FTIR spectrum of Syloid XDP 3050 indicated an intense absorption band at 1067 cm^{-1} that corresponds to the Si–O stretching, which is in accordance with the reported data [64]. Regarding the solidified SNEDDS formula, the resultant FTIR spectrum revealed the appearance of a broad band around 3400 cm^{-1}, indicating superimposed bands of carboxylic O–H stretching of RC and the secondary N–H stretching band of GB. Also, The C=O carbonyl stretching band of CC was shifted from 1751 cm-1 to 1751 cm-1, and a decrease in the intensity of the C=O stretching band of RC at 1545 cm^{-1} was observed. Additionally, a wide and broadband that corresponds to Syloid XDP 3050 was detected at its original position but covering the C-H bands of the tested compounds.

SEM

The scanning electron microscopy (SEM) images of the APIs powders (RC, GB, and CC) and the solidifier (Syloid XDP 3050), as well as the solidified SNEDDS formula, are depicted in Fig. 6 at high magnification power to investigate their surfaces' properties. The results showed evidence of the low crystallinity of RC and the crystalline nature of both GB and CC, which is in accordance with the data obtained in the PXRD section. Syloid XDP 3050 particles were noticed at a size range of around 30 μm, with smooth surfaces. The SEM of the solidified SNEDDS formula indicated the presence of the solidified SNEDDS particles on the surfaces of Syloid, and upon more magnification (10,000 x) small irregular particles in the nanosize range around were observed scattered on the surfaces of Syloid particles, indicating SNEDDS globules solidified with Syloid. The obtained results are in agreement with FTIR and PXRD data confirming the presence of drugs in the amorphous state [65].
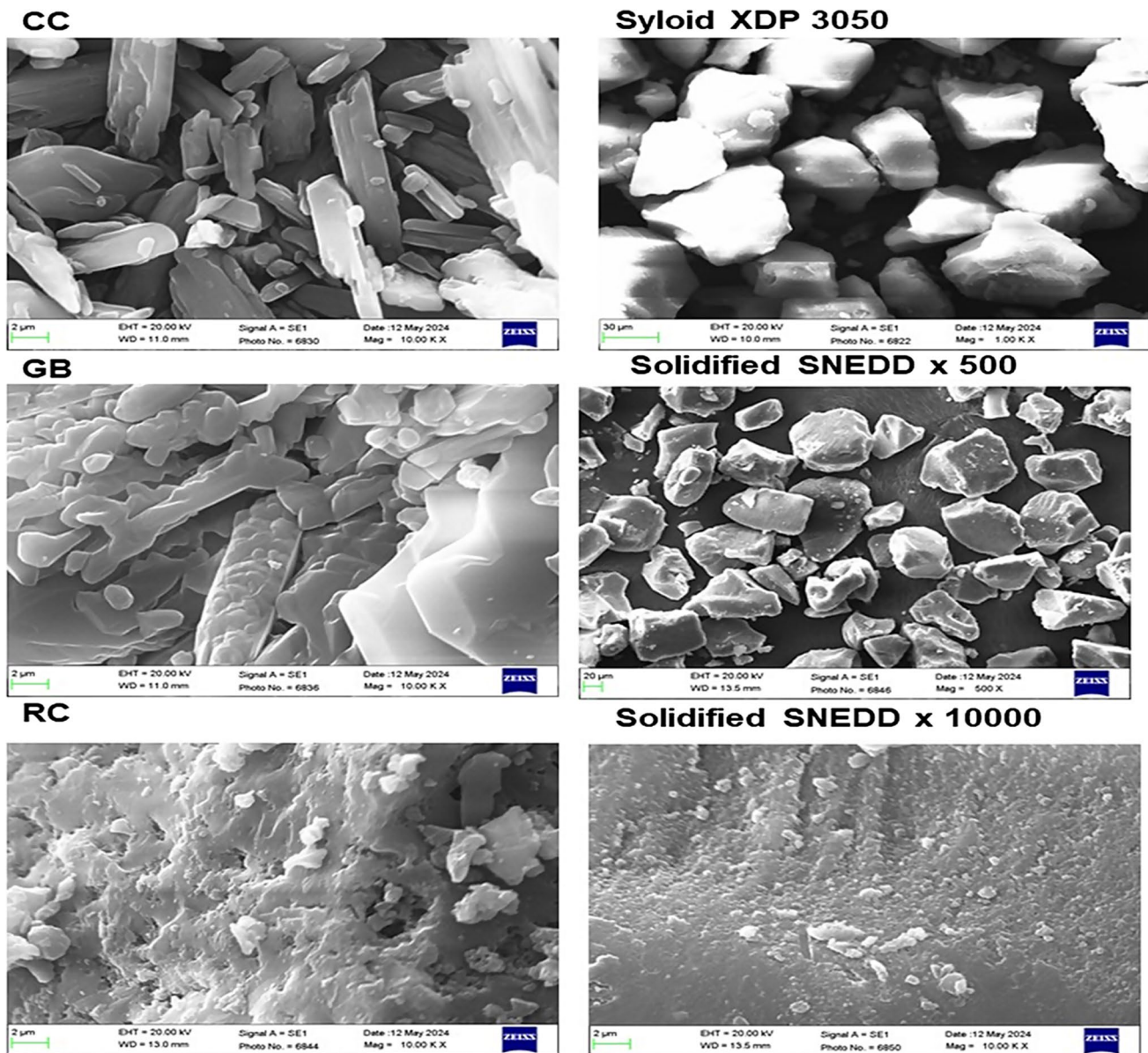
Fig. 6 SEM images of SNEDDS formula containing RC, GB and CC and solidified with Syloid XDP 350 compared to the individual components

Conclusion

The present study shows that the prepared solidified supersaturated SNEDDS formulation is considered as an effective delivery system for CC, GB, and RC. The incorporation of PVP-K30 as a supersaturated agent in the SNEDDS formulation boosts the solubility of poorly water-soluble drugs, which could ensure better therapeutic efficacy. Overall, the proposed triple combination therapy using solid supersaturated SNEDDS holds open a new opportunity to enhance therapeutic outcomes in patients diagnosed with metabolic syndrome. Further *in-vivo* studies are vital to assess the influence of prepared formulation on the oral bioavailability and therapeutic efficacy of loaded triple therapy.

Author Contributions Conceptualization, A.Y.S, M.A.I.; methodology, A.Y.S., M.A.I., D.H.A., A.J.; software, A.Y.S., M.A.I., D.H.A.;validation, A.Y.S., M.A.I., D.H.A.; formal analysis, A.Y.S., M.A.I., D.H.A.; investigation, A.Y.S., M.A.I., D.H.A., A.J.; resources, M.A.I.; data curation, A.Y.S., D.H.A.; writing—original draft preparation, A.Y.S., M.A.I., D.H.A.; writing—review and editing, A.Y.S., M.A.I.; visualization, A.Y.S., M.A.I., D.H.A.; supervision, M.A.I.;

Declarations

Conflicts of Interest The authors declare no conflict of interest.

References

1. Ambroselli D, Masciulli F, Romano E, Catanzaro G, Besharat ZM, Massari MC, et al. New Advances in Metabolic Syndrome, from Prevention to Treatment: The Role of Diet and Food. Nutrients. 2023;15(3):640.

2. Wang HH, Lee DK, Liu M, Portincasa P, Wang DQ-H. Novel insights into the pathogenesis and management of the metabolic syndrome. Pediatr Gastroenterol Hepatol Nutr. 2020;23(3):189.

3. Saklayen MG. The global epidemic of the metabolic syndrome. Curr Hypertens Rep. 2018;20(2):1–8.

4. Lemieux I, Després J-P. Metabolic syndrome: Past, present and future. MDPI. 2020;12:3501.

5. Mohamed SM, Shalaby MA, El-Shiekh RA, El-Banna HA, Emam SR, Bakr AF. Metabolic syndrome: risk factors, diagnosis, pathogenesis, and management with natural approaches. Food Chemistry Advances. 2023;3: 100335.

6. Castro-Barquero S, Ruiz-León AM, Sierra-Pérez M, Estruch R, Casas R. Dietary strategies for metabolic syndrome: a comprehensive review. Nutrients. 2020;12(10):2983.

7. National Institutes of Health [Aviable from: https://www.nhlbi.nih.gov/health/metabolic-syndrome/treatment]. Accessed 6 Jan 2024.

8. Rask Larsen J, Dima L, Correll CU, Manu P. The pharmacological management of metabolic syndrome. Expert Rev Clin Pharmacol. 2018;11(4):397–410.

9. LM Swislocki A, Siegel D, Jialal I. Pharmacotherapy for the metabolic syndrome. Curr Vasc Pharmacol. 2012;10(2):187-205.

10. Chi Y, Xu W, Yang Y, Yang Z, Lv H, Yang S, et al. Three candesartan salts with enhanced oral bioavailability. Cryst Growth Des. 2015;15(8):3707–14.

11. Povlsen AL, Grimm D, Wehland M, Infanger M, Krüger M. The vasoactive Mas receptor in essential hypertension. J Clin Med. 2020;9(1):267.

12. Prasad A, Quyyumi AA. Renin-angiotensin system and angiotensin receptor blockers in the metabolic syndrome. Circulation. 2004;110(11):1507–12.

13. Badila E, Frunza SA, Tirziu CM, Bartos D, Dorobantu M. The effect of candesartan on blood pressure, metabolic profile and renal function in hypertensive patients. Int J Cardiol. 2009;137:S134–5.

14. Menikdiwela KR, Ramalingam L, Rasha F, Wang S, Dufour JM, Kalupahana NS, et al. Autophagy in metabolic syndrome: breaking the wheel by targeting the renin–angiotensin system. Cell Death Dis. 2020;11(2):87.

15. Albertini B, Sabatino MD, Melegari C, Passerini N. Formulation of spray congealed microparticles with self-emulsifying ability for enhanced glibenclamide dissolution performance. J Microencapsul. 2015;32(2):181–92.

16. Lucio D, Irache JM, Font M, Martínez-Ohárriz MC. Supramolecular structure of glibenclamide and β-cyclodextrins complexes. Int J Pharm. 2017;530(1–2):377–86.

17. Khan S, Madni A, Rahim MA, Shah H, Jabar A, Khan MM, et al. Enhanced *in vitro* release and permeability of glibenclamide by proliposomes: Development, characterization and histopathological evaluation. J Drug Deliv Sci Technol. 2021;63: 102450.

18. Franco CC, Prates KV, Previate C, Moraes AM, Matiusso CC, Miranda RA, et al. Glibenclamide treatment blocks metabolic dysfunctions and improves vagal activity in monosodium glutamate-obese male rats. Endocrine. 2017;56:346–56.

19. Schelz Z, Muddather HF, Zupkó I. Repositioning of HMG-CoA Reductase Inhibitors as Adjuvants in the Modulation of Efflux Pump-Mediated Bacterial and Tumor Resistance. Antibiotics. 2023;12(9):1468.

20. Pierzchlińska A, Droździk M, Białecka M. A possible role for HMG-CoA reductase inhibitors and its association with HMGCR genetic variation in Parkinson's disease. Int J Mol Sci. 2021;22(22):12198.

21. Stalenhoef AF, Ballantyne CM, Sarti C, Murin J, Tonstad S, Rose H, et al. A comparative study with rosuvastatin in subjects with metabolic syndrome: results of the COMETS study. Eur Heart J. 2005;26(24):2664–72.

22. Deedwania PC, Hunninghake DB, Bays HE, Jones PH, Cain VA, Blasetto JW, et al. Effects of rosuvastatin, atorvastatin, simvastatin, and pravastatin on atherogenic dyslipidemia in patients with characteristics of the metabolic syndrome. Am J Cardiol. 2005;95(3):360–6.

23. Bostan C, Yildiz A, Ozkan AA, Uzunhasan I, Kaya A, Yigit Z. Beneficial effects of rosuvastatin treatment in patients with metabolic syndrome. Angiology. 2015;66(2):122–7.

24. Asrani S, Bacharach J, Holland E, McKee H, Sheng H, Lewis RA, et al. Fixed-dose combination of netarsudil and latanoprost in ocular hypertension and open-angle glaucoma: pooled efficacy/safety analysis of phase 3 MERCURY-1 and-2. Adv Ther. 2020;37:1620–31.

25. Gleiter CH, Mörike KE. Clinical pharmacokinetics of candesartan. Clin Pharmacokinet. 2002;41:7–17.

26. Obaidat A, Ababneh N. Improvement of glibenclamide bioavailability using cyclodextrin inclusion complex dispersed in polyethylene glycol. Jordan J Pharm Sci. 2009;2(2).

27. Alshora DH, Ibrahim MA, Elzayat E, Almeanazel OT, Alanazi F. Rosuvastatin calcium nanoparticles: improving bioavailability by formulation and stabilization codesign. PLoS ONE. 2018;13(7): e0200218.

28. Kumar S, Singh P. Various techniques for solubility enhancement: An overview. Pharma Innovation. 2016;5(1, Part A):23.

29. Hart ML, Do D, Ansari R, Rizvi S. Brief overview of various approaches to enhance drug solubility. J Dev Drugs. 2013;2(03).

30. Rocha B, de Morais LA, Viana MC, Carneiro G. Promising strategies for improving oral bioavailability of poor water-soluble drugs. Expert Opin Drug Discov. 2023;18(6):615–27.

31. Date AA, Desai N, Dixit R, Nagarsenker M. Self-nanoemulsifying drug delivery systems: formulation insights, applications and advances. Nanomedicine. 2010;5(10):1595–616.

32. Cherniakov I, Domb AJ, Hoffman A. Self-nano-emulsifying drug delivery systems: an update of the biopharmaceutical aspects. Expert Opin Drug Deliv. 2015;12(7):1121–33.

33. Ibrahim MA, Sherif AY, Alshora D, Alsaadi B. A Robust and Reliable UPLC Method for the Simultaneous Quantification of Rosuvastatin Calcium, Glibenclamide, and Candesartan Cilexetil. Separations. 2024;11(4):113.

34. Alhasani KF, Kazi M, Ibrahim MA, Shahba AA, Alanazi FK. Self-nanoemulsifying ramipril tablets: A novel delivery system for the enhancement of drug dissolution and stability. Int J Nanomedicine. 2019;5435–48.

35. Sherif AY, Ibrahim MA. Unveiling the Superiority of Innovative Carbonated Self-Nanoemulsifying Drug Delivery Systems in Improving the Stability of Acid-Labile Drugs: Atorvastatin as a Model Drug. Processes. 2024;12(6):1169.

36. Kazi M, Alhajri A, Alshehri SM, Elzayat EM, Al Meanazel OT, Shakeel F, et al. Enhancing oral bioavailability of apigenin using a bioactive self-nanoemulsifying drug delivery system (Bio-SNEDDS): *In vitro*, *in vivo* and stability evaluations. Pharmaceutics. 2020;12(8):749.

37. Shahba AA-W, Sherif AY, Elzayat EM, Kazi M. Combined Ramipril and Black Seed Oil Dosage Forms Using Bioactive Self-Nanoemulsifying Drug Delivery Systems (BIO-SNEDDSs). Pharmaceuticals. 2022;15(9):1120.

38. Alshora D, Ibrahim M, Alanazi N, Alowyid M, Alnakhli ZA, Alshiban NM, et al. Formulation of Glibenclamide proniosomes for oral administration: Pharmaceutical and pharmacodynamics evaluation. Saudi Pharmaceutical Journal. 2023;31(12): 101830.

39. Elzayat EM, Sherif AY, Nasr FA, Attwa MW, Alshora DH, Ahmad SF, et al. Enhanced Codelivery of Gefitinib and Azacitidine for Treatment of Metastatic-Resistant Lung Cancer Using Biodegradable Lipid Nanoparticles. Materials. 2023;16(15):5364.

40. Alshora DH, Alsaif S, Ibrahim MA, Ezzeldin E, Almeanazel OT, Abou El Ela AES, et al. Co-stabilization of pioglitazone HCL nanoparticles prepared by planetary ball milling: in-vitro and in-vivo evaluation. Pharm Dev Techno. 2020;25(7):845–54.

41. Smail SS, Ghareeb MM, Omer HK, Al-Kinani AA, Alany RG. Studies on surfactants, cosurfactants, and oils for prospective use in formulation of ketorolac tromethamine ophthalmic nanoemulsions. Pharmaceutics. 2021;13(4):467.

42. Li S, Madan P, Lin S. Application of Capmul MCM and caprylic acid for the development of danazol-loaded SEDDS. Pharm Dev Technol. 2015;20(7):886–96.

43. Khan BA, Akhtar N, Khan HMS, Waseem K, Mahmood T, Rasul A, et al. Basics of pharmaceutical emulsions: A review. Afr J Pharm Pharmacol. 2011;5(25):2715–25.

44. Khan AA, Kumar A, Ali J, Sahni JK, Baboota S. Formulation, optimization and characterization of Self Nanoemulsifying Drug Delivery System (SNEDDS) of paclitaxel for solubility enhancement. Nanosci Nanotechnol Lett. 2013;5(8):861–7.

45. Elgart A, Cherniakov I, Aldouby Y, Domb AJ, Hoffman A. Improved oral bioavailability of BCS class 2 compounds by self nano-emulsifying drug delivery systems (SNEDDS): the underlying mechanisms for amiodarone and talinolol. Pharm Res. 2013;30:3029–44.

46. Akiladevi D, Prakash H, Biju G, Madumitha N. Nano-novel approach: Self nano emulsifying drug delivery system (SNEDDS)-Review article. Res J Pharm Technol. 2020;13(2):983–90.

47. Rathore C, Hemrajani C, Sharma AK, Gupta PK, Jha NK, Aljabali AA, et al. Self-nanoemulsifying drug delivery system (SNEDDS) mediated improved oral bioavailability of thymoquinone: optimization, characterization, pharmacokinetic, and hepatotoxicity studies. Drug Deliv Transl Res. 2023;13(1):292–307.

48. Zhao Y, Wang C, Chow AH, Ren K, Gong T, Zhang Z, et al. Self-nanoemulsifying drug delivery system (SNEDDS) for oral delivery of Zedoary essential oil: formulation and bioavailability studies. Int J Pharm. 2010;383(1–2):170–7.

49. Czuba E, Diop M, Mura C, Schaschkow A, Langlois A, Bietiger W, et al. Oral insulin delivery, the challenge to increase insulin bioavailability: Influence of surface charge in nanoparticle system. Int J Pharm. 2018;542(1–2):47–55.

50. Penalva R, Esparza I, Larraneta E, González-Navarro CJ, Gamazo C, Irache JM. Zein-based nanoparticles improve the oral bioavailability of resveratrol and its anti-inflammatory effects in a mouse model of endotoxic shock. J Agric Food Chem. 2015;63(23):5603–11.

51. Patel K, Sarma V, Vavia P. Design and evaluation of lumefantrine–oleic acid self nanoemulsifying ionic complex for enhanced dissolution. DARU J Pharm Sci. 2013;21:1–11.

52. Shahba AA-W, Mohsin K, Alanazi FK, Abdel-Rahman SI. Optimization of self-nanoemulsifying formulations for weakly basic lipophilic drugs: role of acidification and experimental design. Brazilian J Pharm Sci. 2016;52:653–67.

53. Shahba AA, Tashish AY, Alanazi FK, Kazi M. Combined self-nanoemulsifying and solid dispersion systems showed enhanced cinnarizine release in hypochlorhydria/achlorhydria dissolution model. Pharmaceutics. 2021;13(5):627.

54. Craig D, Lievens H, Pitt K, Storey D. An investigation into the physico-chemical properties of self-emulsifying systems using low frequency dielectric spectroscopy, surface tension measurements and particle size analysis. Int J Pharm. 1993;96(1–3):147–55.

55. Kaur G, Chandel P, Harikumar S. Formulation development of self nanoemulsifying drug delivery system (SNEDDS) of celecoxib for improvement of oral bioavailability. Pharmacophore. 2013;4(4–2013):120–33.

56. Nazlı H, Mesut B, Özsoy Y. *In vitro* evaluation of a solid supersaturated self nanoemulsifying drug delivery system (Super-SNEDDS) of aprepitant for enhanced solubility. Pharmaceuticals. 2021;14(11):1089.

57. Alwadei M, Kazi M, Alanazi FK. Novel oral dosage regimen based on self-nanoemulsifying drug delivery systems for code-livery of phytochemicals–Curcumin and thymoquinone. Saudi Pharmaceutical Journal. 2019;27(6):866–76.

58. Alghananim A, Özalp Y, Mesut B, Serakinci N, Özsoy Y, Güngör S. A solid ultra fine self-nanoemulsifying drug delivery system (S-SNEDDS) of deferasirox for improved solubility: optimization, characterization, and *in vitro* cytotoxicity studies. Pharmaceuticals. 2020;13(8):162.

59. Sarfraz RM, Ahmad M, Mahmood A, Ijaz H. Development, *in vitro* and *in vivo* evaluation of pH responsive β-CD-comethacrylic acid-crosslinked polymeric microparticulate system for solubility enhancement of rosuvastatin calcium. Polym-Plast Technol Eng. 2018;57(12):1175–87.

60. Alshadidi A, Shahba AA-W, Sales I, Rashid MA, Kazi M. Combined curcumin and lansoprazole-loaded bioactive solid self-nanoemulsifying drug delivery systems (Bio-SSNEDDS). Pharmaceutics. 2021;14(1):2.

61. Corrie L, Kaur J, Awasthi A, Vishwas S, Gulati M, Saini S, et al. Multivariate data analysis and central composite design-oriented optimization of solid carriers for formulation of curcumin-loaded solid SNEDDS: Dissolution and bioavailability assessment. Pharmaceutics. 2022;14(11):2395.

62. Kapure V, Pande V, Deshmukh P. Dissolution enhancement of rosuvastatin calcium by liquisolid compact technique. J Pharm. 2013;2013(1): 315902.

63. Kamalakkannan V, Puratchikody A, Ramanathan L. Development and characterization of controlled release polar lipid microparticles of candesartan cilexetil by solid dispersion. Research in pharmaceutical sciences. 2013;8(2):125.

64. Al-Oweini R, El-Rassy H. Synthesis and characterization by FTIR spectroscopy of silica aerogels prepared using several Si (OR)4 and R″ Si (OR′)3 precursors. J Mol Struct. 2009;919(1–3):140–5.

65. Inugala S, Eedara BB, Sunkavalli S, Dhurke R, Kandadi P, Jukanti R, et al. Solid self-nanoemulsifying drug delivery system (S-SNEDDS) of darunavir for improved dissolution and oral bioavailability: *in vitro* and *in vivo* evaluation. Eur J Pharm Sci. 2015;74:1–10.